Available online at www.sciencedirect.com
ScienceDirect
International Journal of Heat and Mass Transfer 50 (2007) 257–268
International Journal of HEAT and MASS TRANSFER
www.elsevier.com/locate/ijhmt

Improving convergence of summations in heat conduction

James V. Beck [a,*], Kevin D. Cole [b]

[a] Department of Mechanical Engineering, 2555 Engineering Building, Michigan State University, East Lansing, MI 48824, United States
[b] Department of Mechanical Engineering, N104 Walter Scott Center, University of Nebraska-Lincoln, Lincoln, NE 68588, United States

Received 13 April 2006; received in revised form 16 June 2006
Available online 7 September 2006

Abstract

This paper addresses exact, transient heat-conduction solutions in two-dimensional rectangles heated at a boundary. The standard method of separation of variables (SOV) solution has two parts, steady-state (or quasi-steady) and complementary transient. The steady-state component frequently converges slowly at the heated surface, which is usually the one of greatest interest. New procedures are given to construct a steady solution in the form of a single summation, one having eigenvalues in the homogeneous direction (yielding the same result as the standard SOV solution) and the other having eigenvalues in the non-homogeneous direction (called the non-standard solution). The non-standard solutions have much better convergence behavior at and near the heated boundary than the standard forms. Examples are given.

Keywords: Convergence; Analytical heat conduction; Series identities; Separation of variables

1. Introduction

1.1. Problem description

Exact transient heat conduction solutions in Cartesian coordinates are important for many reasons. One is for the verification of large finite element and finite control volume codes [1]. The insight that these exact solutions provide for modeling simple geometries is also important. Unfortunately, the standard steady-state separation of variables (SOV) component of these solutions may be poorly convergent at the heated surface (the one of greatest interest) for the temperature and even more so for the heat flux. In this paper, steady-state solutions are derived that are much more accurate and better behaved on the heated surface than the standard SOV solutions.

In the standard SOV solution for a transient heat conduction problem in a rectangle with a non-homogeneous boundary condition, the steady-state component of the solution is constructed from an eigenvalue problem in the homogeneous boundary condition direction. The non-standard solution uses eigenvalues in the non-homogeneous direction. For a 2D problem, the standard steady-state SOV solution is a single summation. The long-cotime Green's function (GF) solution produces a double-summation for both the steady-state and transient components of the solution. (The cotime is given by $t-\tau$ and the long cotime GF is derived using SOV.) The steady-state double-summation can be reduced to two different single-summations. One is the standard SOV solution which has eigenvalues in the homogeneous direction. The non-standard solution has eigenvalues in the non-homogeneous direction; it converges much more rapidly at the heated surface than the standard solution.

The steady-state double summation solution discussed in this paper is reduced to a single summation by replacing one of the summations by an algebraic identity. Two general methods of deriving these fundamental algebraic identities are given and many identities are tabulated.

* Corresponding author. Tel.: +1 517 349 6688; fax: +1 517 353 1750.
E-mail address: beck@egr.msu.edu (J.V. Beck).

0017-9310/$ - see front matter © 2006 Elsevier Ltd. All rights reserved.
doi:10.1016/j.ijheatmasstransfer.2006.06.032

Nomenclature

B	boundary condition modifier, used in case identification number system
Bi	Biot number
C_m	$\beta_m W/L$
C_n	$\eta_n L/W$
D	defined by Eq. (15)
G	Green's function (m^{-1}, for 1D form)
h	heat transfer coefficient (W/m^2 °C)
H_1	q_1 for boundary conditions of the 2nd kind, $h_1 T_\infty$ for boundary conditions of the 3rd kind
k	thermal conductivity (W/m °C)
L	length in x-direction (m)
q_1	prescribed heat flux at a boundary (W/m^2)
S	function defined by Eq. (41)
t	time (s)
T	temperature °C
W	length in the y-direction (m)
x, y	spatial variables (m)
X, Y	eigenfunctions and also used in the numbering system

Greek symbols

α	thermal diffusivity (m^2/s)
β	eigenvalue in the x-direction
$\delta(\cdot)$	Dirac delta function
η	eigenvalue in the y-direction
θ	algebraic form of summation, Eq. (13)
ϕ	algebraic form of summation, Eq. (26)
τ	convolution time variable (s)

Subscripts

j	subscript 1 denotes at x (or y) $= 0$, subscript 2 denotes $x = L$
m, n	counting integers for eigenvalues in the x- and y-directions, respectively

Superscript

$+$	denotes a dimensionless quantity

1.2. Literature review

Appropriate heat conduction literature is discussed next in the areas of SOV solutions, alternate solutions, and the uses of alternate solutions. The standard SOV procedure for steady-state 2D (and 3D) heat conduction is the one currently recommended in graduate heat conduction books. For example, Arpaci [2], Ozisik [3], Kakac and Yener [4] and Gebhart [5] clearly state that this is the proper way to solve these problems. Incropera and DeWitt [6] appear to be in agreement with these authors.

Alternate solutions have been known for many years [7]. The non-standard results can be constructed with several methods, including the variation of parameters method [8] and the steady-state GF method [9,10]. A technique used by applied mathematicians "simply" subtracts the 1D solution in the non-homogeneous direction. This is a powerful technique but it usually transforms the problem from a single boundary value problem to two or more boundary value problems. The procedure may not be obvious, however; an example of such a derivation is the one used to obtain Eqs. (7a,b) in [1].

The time-partitioning method, which was developed for transient problems, can also be used to construct a rapidly-convergent steady-state temperature solution (in the limit as time becomes large). The time-partitioning method involves both large-cotime series-form GF and small-cotime series-form GF, each of which converges well in their respective time range [12, Chapter 5, 13–15]. In contrast, the new procedure discussed in this paper is easier to implement than the time-partitioning method, in part because only the long-cotime GF is used. As presented in [11] the time-partitioning method for 2D and 3D problems also involves a numerical integration of the small cotime GFs, which is a disadvantage. Even so, it may be more numerically efficient than the proposed method; that remains to be investigated. However, numerical efficiency may not be important with the present computers but accuracy must be assured for verification.

A number of other techniques have been employed for exact solution of heat conduction problems. De Monte [16,17] has written a number of papers on multi-dimensional multi-layer materials and is a proponent of the "natural" analytic method. Lu and co-authors [18,19] have also written a number of papers for multi-layer slabs and cylinders; in [18] they approximate time-varying boundary conditions with temporal sinusoids. Another type of heat conduction problem involves semi-infinite geometries [20]. The number of analytical heat conduction solution papers is exceeded by the papers on inverse heat conduction; examples are the recent papers [21,22].

There are a number of uses of alternate forms of heat conduction solutions. A primary reason is that heat conduction solutions are not uniformly convergent. As mentioned above, the standard SOV approach produces series solutions that converge very slowly at the location of greatest interest, namely, near the surface with the non-homogeneous condition [1]. Where the standard solution converges slowly, an alternate solution may converge many times faster [1,9,13]. Another use of alternate solutions is intrinsic verification [11] which is a basic feature of the time-partitioning method. When the partition time

is varied over acceptable cotimes, the same numerical values (to as many significant figures as desired) are obtained. This provides a very powerful means of verification. The proposed herein method also provides intrinsic verification by using multiple solutions which can then be compared [11]. However, the proposed procedure does not have a single parameter analogous to the partition time, which can be continuously varied.

1.3. Outline

This paper is divided into several sections. The problem is formulated in Section 2 for the transient heat conduction in the rectangle heated at the $x = 0$ surface, with the GF solution given in the form of a double-summation (which can be extended to the parallelepiped with a triple summation). From the double-summation, two alternate single-sum solutions are constructed by studying a one-dimensional transient problem, first along the y-direction (homogeneous direction, Section 3), and second along the x-direction (non-homogeneous direction, Section 4). The first of these, which we call non-standard, reduces the double summation to a single summation having eigenvalues in the x-direction (non-homogeneous direction). The second way, called the standard solution, produces a result which has the eigenvalues in the y-direction (homogeneous direction). (To remember this, note that the non-standard procedure produces a 1D summation with eigenvalues in the non-homogeneous direction.) Section 5 provides some numerical results and a comparison of the methods. A discussion in Section 6 is also given to show that the new method of removing a summation is equivalent to using a steady-state, 1D, fin-type GF.

2. Problem formulation

An example is given to illustrate reducing the double summations to a single summation in the steady-state portion of the GF solution in transient heat conduction in a homogeneous rectangle. (The same principle applies to reducing a triple summation in a 3D problem to a double summation.) Consider the general transient heat conduction problem denoted $XIJB(y\text{-})0\,YKLB00T0$ (see [12, Chapter 2] for a full discussion of the numbering system for heat conduction.). This problem has a single non-homogeneous term at boundary $x = 0$; it can be prescribed temperature, prescribed heat flux, and prescribed convection conditions, denoted the first, second and third kinds of boundary conditions, respectively. Specifically, the I, J, K and L values can be 1, 2 or 3 corresponding to the boundary condition kinds. This designation leads in part to the numbering system. A general variation in y-direction of the non-homogeneous boundary condition at the $x = 0$ face is permitted.

A mathematical statement of the above linear heat conduction problem is

$$\frac{\partial^2 T}{\partial x^2}+\frac{\partial^2 T}{\partial y^2}=\frac{1}{\alpha}\frac{\partial T}{\partial t},\quad 0<x<L,\quad 0<y<W,\ t>0 \tag{1a}$$

$$-k\tfrac{\partial T}{\partial x}(0,y,t)=q_1 f(y) \text{ or } h_1[T_\infty f(y)-T(0,y,t)]$$
Boundary conditions at $x = L,\ y = 0,\ W$ are homogeneous
Initial condition: $T(x,y,0)=0$ (1b)

Using GFs the solution can be written as

$$T(x,y,t)=\frac{\alpha}{k}H_1\int_{\tau=0}^{t}G_{XIJ}(x,0,t-\tau)\times\int_{y'=0}^{W}f(y')G_{YKL}(y,y',t-\tau)\,\mathrm{d}y'\,\mathrm{d}\tau \tag{2}$$

In the following discussion, for $I = 2$ (that is, boundary condition of the second kind), $H_1 = q_1$; for $I = 3$ (boundary condition of the third kind), $H_1 = h_1 T_{\mathbb{N}}$. (For $I = 1$ (boundary condition of the first kind), the following development is more affected: replace $(H_1/k)G_{X1J}$ by $T_1\partial G_{X1J}/\partial x'$.) Let the long cotime GFs be used; they are

$$G_{XIJ}(x,0,t-\tau)=\sum_{m=0}^{\infty}\frac{\mathrm{e}^{-\beta_m^2\frac{\alpha(t-\tau)}{L^2}}}{N_{x,m}}X_m(x)X_m(0) \tag{3a}$$

$$G_{YKL}(y,y',t-\tau)=\sum_{n=0}^{\infty}\frac{\mathrm{e}^{-\eta_n^2\frac{\alpha(t-\tau)}{W^2}}}{N_{y,n}}Y_n(y)Y_n(y') \tag{3b}$$

where X_m and Y_n are eigenfunctions, and N_x and N_y are norms, constructed from Fourier series, with the precise form determined by the specific boundary conditions present. See [12, p. 99] for a complete list. Performing the integrations in Eq. (2) yields

$$T(x,y,t)=\frac{1}{k}H_1\sum_{m=0}^{\infty}\sum_{n=0}^{\infty}\times\frac{X_m(x)X_m(0)Y_n(y)IY_n}{N_{x,m}N_{y,n}\left[\left(\frac{\beta_m}{L}\right)^2+\left(\frac{\eta_n}{W}\right)^2\right]}\left(1-\mathrm{e}^{-\left[\left(\frac{\beta_m}{L}\right)^2+\left(\frac{\eta_n}{W}\right)^2\right]\alpha t}\right) \tag{4a}$$

where

$$IY_n=\int_{y'=0}^{W}f(y')Y_n(y')\,\mathrm{d}y' \tag{4b}$$

The solution given by Eq. (4a) can be written in the form

$$T(x,y,t)=\left\{\begin{array}{l}\frac{1}{k}H_1\sum_{m=0}^{\infty}\sum_{n=0}^{\infty}\frac{X_m(x)X_m(0)Y_n(y)IY_n}{N_{x,m}N_{y,n}\left[\left(\frac{\beta_m}{L}\right)^2+\left(\frac{\eta_n}{W}\right)^2\right]}\\ -\frac{1}{k}H_1\sum_{m=0}^{\infty}\sum_{n=0}^{\infty}\frac{X_m(x)X_m(0)Y_n(y)IY_n}{N_{x,m}N_{y,n}\left[\left(\frac{\beta_m}{L}\right)^2+\left(\frac{\eta_n}{W}\right)^2\right]}\mathrm{e}^{-\left[\left(\frac{\beta_m}{L}\right)^2+\left(\frac{\eta_n}{W}\right)^2\right]\alpha t}\end{array}\right\} \tag{5}$$

This solution has two major components. The first is the steady-state or quasi-steady component and second is the complementary transient. The more difficult part to evaluate numerically is the steady-state component. It converges algebraically while the complementary transient converges exponentially.

We wish to reduce the double summation to a single summation in the steady-state component by using the following procedure: identify a 1D problem that has a series solution identical to one sum in the double-sum 2D solution; solve this 1D problem to obtain an algebraic solution; and, substitute this algebraic solution for one summation. This procedure can be used to obtain two different single-summation solutions which are equivalent mathematically but they usually converge properties quite differently. In the next section a 1D transient problem along the y-direction is examined as part of this procedure; it produces the non-standard solution.

3. Non-homogeneous direction 1D eigenvalue problem (non-standard solution)

We now obtain a 1D solution from Eq. (2) by replacing one of the GFs by a time dependent term of that series. That can be done for either of the two GFs to obtain two different 1D problems. Consider now a 1D problem in the y-direction that is formed by replacing G_{XIJ} in Eq. (2) with a typical transient term, $\exp(-\beta_m^2\alpha(t-\tau)/L^2)$. This analysis results in the eigenvalues in the final single summation being associated with the non-homogeneous direction and thus is nonstandard. It is convenient to divide G_{XIJ} by W since the GF has units of reciprocal length. The result is

$$\begin{aligned} T(y,t) &= \frac{\alpha}{k} H_1 \int_{\tau=0}^{t} \frac{e^{-\left(\frac{\beta_m}{L}\right)^2 \alpha(t-\tau)}}{W} \int_{y'=0}^{W} f(y') G_{YKL}(y,y',t-\tau)\,dy'\,d\tau \\ &= \frac{\alpha}{k}\frac{H_1}{W} e^{-\left(\frac{\beta_m}{L}\right)^2 \alpha t} \int_{\tau=0}^{t} \int_{y'=0}^{W} e^{\left(\frac{\beta_m}{L}\right)^2 \alpha\tau} f(y') G_{YKL}(y,y',t-\tau)\,dy'\,d\tau \end{aligned} \tag{6}$$

The second line of Eq. (6) is recognized as $\exp(-\beta_m^2\alpha t/L^2)$ multiplied by a temperature. This temperature, denoted T' below, is for a volumetric energy generation problem. (see the second line of Eq. (3.16) of [12]). The two boundary conditions are homogeneous and are of the Kth kind at $y=0$ and of the Lth kind at $y=W$. Both K and L can go from 1 to 3, for a total of nine cases. The volume energy generation (with units of W/m^3) for T' is exponentially increasing in time as

$$g = \frac{H_1}{W} e^{\left(\frac{\beta_m}{L}\right)^2 \alpha t} f(y) \tag{7}$$

The 1D conduction equation driven by this heating term is

$$\begin{aligned} &\frac{\partial^2 T'}{\partial y^2} + \frac{H_1/W}{k} f(y) e^{\left(\frac{\beta_m}{L}\right)^2 \alpha t} = \frac{1}{\alpha}\frac{\partial T'}{\partial t}, \\ &T'(y,t) = e^{\left(\frac{\beta_m}{L}\right)^2 \alpha t} T(y,t) \end{aligned} \tag{8}$$

This case is described by the notation $YKLB00G(y{-}t4)T0$. The boundary conditions are identical to the homogeneous boundary conditions from the original 2D problem (Kth kind at $y=0$ and Lth kind at $y=W$). The GF solution (using the long cotime form) for this problem may be written [12, p.43]

$$\begin{aligned} T'(y,t) &= \frac{\alpha}{k}\frac{H_1}{W} e^{\left(\frac{\beta_m}{L}\right)^2 \alpha t} \int_{u=0}^{t} \sum_{n=0}^{\infty} e^{-\left(\frac{\beta_m}{L}\right)^2 \alpha u} e^{-\eta_n^2 \frac{\alpha u}{W^2}} \frac{Y_n(y) I Y_n}{N_{y,n}}\,du \\ &= \frac{1}{k}\frac{H_1}{W} e^{\left(\frac{\beta_m}{L}\right)^2 \alpha t} \sum_{n=0}^{\infty} \frac{Y_n(y) I Y_n}{N_{y,n}\left[\left(\frac{\beta_m}{L}\right)^2 + \left(\frac{\eta_n}{W}\right)^2\right]} \\ &\quad \times \left(1 - e^{-\left[\left(\frac{\beta_m}{L}\right)^2 + \left(\frac{\eta_n}{W}\right)^2\right]\alpha t}\right) \end{aligned} \tag{9}$$

Note that the summation above is identical in form to that in the 2D solution given by Eq. (4a). A main difference is the multiplication by an exponentially increasing function of time.

To isolate the summation from that multiplicative term, consider the following transformation:

$$T'(y,t) = \frac{H_1 W}{k} e^{\left(\frac{\beta_m}{L}\right)^2 \alpha t} \theta_m(y,t) \tag{10}$$

Introducing this equation into Eq. (8) gives

$$\frac{\partial^2 \theta_m}{\partial (y^+)^2} + f(y) = \frac{W^2}{\alpha}\frac{\partial \theta_m}{\partial t} + C_m^2 \theta_m \tag{11}$$

where $y^+ = y/W$ and $C_m = \beta_m W/L$. The dimensionless quantity θ_m has a steady-state solution which is the one we seek. The steady-state describing equation for θ_m is

$$\frac{d^2\theta_m}{d(y^+)^2} - C_m^2 \theta_m + f(y) = 0 \tag{12}$$

The function θ_m satisfies homogeneous boundary conditions corresponding to the Kth kind at $y=0$ and Lth kind at $y=W$ (identical to the original 2D temperature problem). Several methods are available to solve this second-order ordinary differential equation for θ_m. However, it is convenient to use symbolic manipulation software. We will show later that the steady 1D GF can also be used. The important point is that a non-series solution can be found for $\theta_m(y)$, in the form of an algebraic expression for simple $f(y)$ functions. Expressions for $\theta_m(y)$ for $f(y)=1$ are given in Appendix A. A comparison between Eqs. (9) and (10) indicates that $\theta_m(y)$ can be written in the series form of

$$\theta_m(y) = \frac{1}{W^2} \sum_{n=0}^{\infty} \frac{Y_n(y) I Y_n}{N_{y,n}\left[\left(\frac{\beta_m}{L}\right)^2 + \left(\frac{\eta_n}{W}\right)^2\right]} \tag{13}$$

which is dimensionless. Now examine the steady-state component of Eq. (5) to isolate the series form of $\theta_m(y)$ given by Eq. (13)

$$T(x,y) = \sum_{m=0}^{\infty} \left\{ \frac{H_1 W^2}{k} \frac{1}{W^2} \sum_{n=0}^{\infty} \frac{Y_n(y) I Y_n}{N_{y,n}\left[\left(\frac{\beta_m}{L}\right)^2 + \left(\frac{\eta_n}{W}\right)^2\right]} \right\} \frac{X_m(x) X_m(0)}{N_{x,m}} \tag{14a}$$

Finally, replace the series form of $\theta_m(y)$ by the non-series form to get

$$T(x,y)=\frac{H_1W^2}{k}\sum_{m=0}^{\infty}\theta_m(y)\frac{X_m(x)X_m(0)}{N_{x,m}} \tag{14b}$$

The double sum for the 2D steady temperature is replaced by a single sum. This result has eigenfunctions in the non-homogeneous direction. Hence it is a non-standard result. The above development involved a non-homogeneous boundary of the second or third kind at $x=0$, but a similar approach is used for a boundary condition of the first kind.

The result given by Eq. (14b) can be obtained using other methods, but this method produces a small number of general identities that can be used for many cases, including 3D problems. A general result is given in Appendix A which is

$$\theta_m(y)=\frac{1}{C_m^2}\left[1-\frac{D_{B1}\left(e^{-C_m y^+}+D_2e^{-C_m(2-y^+)}\right)+D_{B2}\left(e^{-C_m(1-y^+)}+D_1e^{-C_m(1+y^+)}\right)}{1-D_1D_2e^{-2C_m}}\right]$$
$$D_j=(C_m-Bi_j)/(C_m+Bi_j),\quad D_{Bj}=Bi_j/(C_m+Bi_j),\quad j=1,2 \tag{15}$$

where $Bi_1=h_{y1}W/k$, $Bi_2=h_{y2}W/k$ and the heat transfer coefficients, h_{y1} and h_{y2}, are at $y=0$ and W, respectively. Table 1 lists the D coefficients for K, $L=1$, 2, 3 (nine cases), which have values in the intervals $-1\leqslant D_j\leqslant 1$ and $0\leqslant D_{Bj}\leqslant 1$. Also note the last column of this table; it provides simple expressions for the limiting cases of C_m going to zero. Notice that although the eigenvalues in the series for boundary conditions of the third kind (see Eq. (A.3)) are not easy to evaluate, no eigenvalues are required using Eq. (15). The range of the $\theta_m(y)$ values is from zero to infinity; however, only the $YF22$, $YF23$, $YF32$ and $YF33$ cases have values greater than one. As m is increased in value, C_m increases and the $\theta_m(y)$ numerical values decrease. A plot of the limiting cases is given in Fig. 1 as a function of y^+; for cases requiring a Biot value, $Bi=1$ is selected. Another important point regarding Eq. (15) is that each case contains additive term $1/C_m^2$ which represents a 1D component in the solution and aids in convergence of the series.

A specific example is given next to demonstrate the method. Consider case $X21B10Y21B00T0$, which includes a boundary condition of the second kind at $y=0$ and of the first kind at $x=L$ and $y=W$. The heat flux is uniform over the $x=0$ surface so that $f(y)=1$. The needed solution for $\theta_m(y)$ is case $YF21B00G1$in Appendix A. (Notice the common element of $Y21B00$ in the notation with $X21B10Y21B00T0$.) The expression for $\theta_m(y)$ is

$$\theta_m(y)=\frac{1}{C_m^2}\left[1-\frac{e^{-C_m(1-y^+)}+e^{-C_m(1+y^+)}}{1+e^{-2C_m}}\right] \tag{16}$$

It is important to observe that this same expression can be used for many other cases. For example, the $X21B10$ could be replaced by $XIJB10$ or $XIJB01$ where I and J can be 1, 2 and 3. Introducing Eq. (16) for $\theta_m(y)$ into Eq. (14b) and using the eigenfunctions for the X21 problem gives the non-standard result of

$$T(x,y)=\frac{q_1L}{k}2\sum_{m=1}^{\infty}\left[1-\frac{e^{-\beta_m\frac{W}{L}(1-y^+)}+e^{-\beta_m\frac{W}{L}(1+y^+)}}{1+e^{-2\beta_m\frac{W}{L}}}\right]\frac{\cos(\beta_m x^+)}{\beta_m^2}$$
$$=\frac{q_1W}{k}\frac{L}{W}\left\{1-x^+-2\sum_{m=1}^{\infty}\frac{e^{-\beta_m\frac{W}{L}(1-y^+)}+e^{-\beta_m\frac{W}{L}(1+y^+)}}{1+e^{-2\beta_m\frac{W}{L}}}\frac{\cos(\beta_m x^+)}{\beta_m^2}\right\} \tag{17a}$$

where the following identity is used:

$$2\sum_{m=1}^{\infty}\frac{\cos(\beta_m\frac{x}{L})}{\beta_m^2}=1-\frac{x}{L},\quad \beta_m=\left(m-\frac{1}{2}\right)\pi \tag{17b}$$

Eq. (17a) converges exponentially for all values of x^+ and all values of y^+ provided y^+ is not near 1. A conservative limit of the maximum number of series terms needed to obtain a given accuracy is to require the smallest magnitude exponent in the numerator of Eq. (17a) to be less than some value. For example, to obtain $\exp(-R)=A$ with $A=10^{-5}$ and 10^{-10}, requires exponent values $R=11.5$ and 23, respectively. From Eq. (17a) we obtain

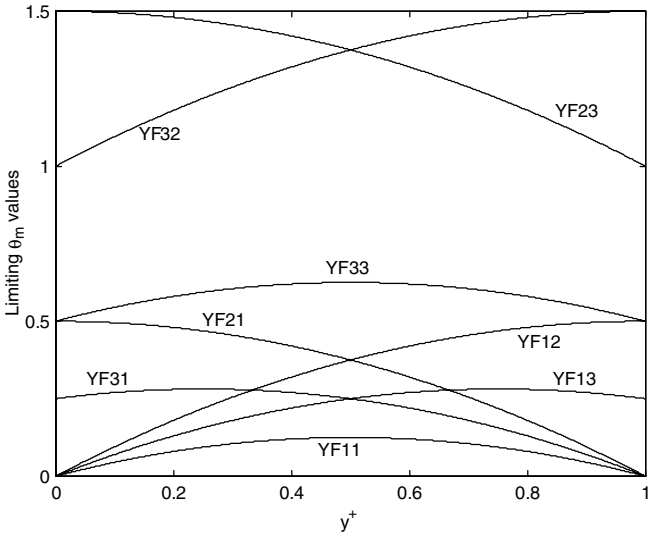

Fig. 1. Limiting values for $\theta_m(y^+)$ as C_m goes to zero. For the $YF13$, $YF23$, $YF31$, $YF32$ and $YF33$ cases, the Bi numbers are 1.0.

Table 1
Coefficients for special cases coming from case $YF33B00G1$ given by Eq. (A.4)

Number	D_1	D_{B1}	D_2	D_{B2}	$\lim_{C_m\to 0}\theta_m(y^+)$
$YF11$	-1	1	-1	1	$(y^+/2)(1-y^+)$
$YF12$	-1	1	1	0	$(y^+/2)(2-y^+)$
$YF13$	-1	1	D_2	D_{B2}	$\frac{y^+}{2}\frac{2-y^+ +Bi_2(1-y^+)}{1+Bi_2}$
$YF21$	1	0	-1	1	$\frac{1}{2}(1-(y^+)^2)$
$YF22$	1	0	1	0	∞
$YF23$	1	0	D_2	D_{B2}	$\frac{1}{2}(1-(y^+)^2)+\frac{1}{Bi_2}$
$YF31$	D_1	D_{B1}	-1	1	$\frac{1-y^+}{2}\frac{1+y^+ +Bi_1y^+}{1+Bi_1}$
$YF32$	D_1	D_{B1}	1	0	$\frac{y^+}{2}(2-y^+)+\frac{1}{Bi_1}$
$YF33$	D_1	D_{B1}	D_2	D_{B2}	For $Bi_1=Bi_2=Bi$: $\frac{y^+}{2}(1-y^+)+\frac{1}{2Bi}$

$$\left(m_{\max}-\frac{1}{2}\right)\pi\frac{W}{L}(1-y^+)=R,$$
$$m_{\max}=\frac{R}{\pi(1-y^+)}\frac{L}{W}+\frac{1}{2} \tag{18a}$$

Note that more terms are needed as L/W is increased. For $R=11.5$ and $L/W=1$, the maximum number of terms is

$$m_{\max}=\frac{3.66}{1-y^+}+\frac{1}{2} \tag{18b}$$

If $y^+=0$, only four terms in the summation is needed to obtain relative accuracies of better than 10^{-5}. Surprisingly for accuracies to 10^{-10}, only seven terms are needed for $y^+=0$. That means that the error divided by 100,000 requires only about twice as many terms, which is a demonstration of exponential convergence.

4. Homogeneous direction 1D eigenvalue problem (standard solution)

A similar method is used to obtain a result which is identical to that produced by the standard SOV procedure which produces a single summation with the eigenvalues directed in the homogeneous direction. We now replace the double sum of the 2D problem given by Eq. (2) with a single sum for a 1D problem in the x-direction. That is accomplished by replacing G_{YKL} in Eq. (2) with a typical transient term, $\exp(-\eta_n^2\alpha(t-\tau)/W^2)$

$$\begin{aligned}T_{1D}(x,t)&=\frac{\alpha}{k}H_1\int_{\tau=0}^{t}G_{XIJ}(x,0,t-\tau)\mathrm{e}^{-\left(\frac{\eta_n}{W}\right)^2\alpha(t-\tau)}\,\mathrm{d}\tau\\&=\frac{\alpha}{k}H_1\mathrm{e}^{-\left(\frac{\eta_n}{W}\right)^2\alpha t}\int_{\tau=0}^{t}G_{XIJ}(x,0,t-\tau)\mathrm{e}^{\left(\frac{\eta_n}{W}\right)^2\alpha\tau}\,\mathrm{d}\tau\end{aligned} \tag{19}$$

The solution in the second line is the temperature for an exponentially increasing heat flux boundary condition at $x=0$; it is also multiplied by a decaying exponential. Let the solution without the decaying exponential be termed T'. The boundary condition of the second kind at $x=0$ is described mathematically by

$$-k\frac{\partial T'}{\partial x}(0,t)=q_1\mathrm{e}^{\left(\frac{\eta_n}{W}\right)^2\alpha t} \tag{20a}$$

This problem is denoted $X2JB40T0$, where the "4" denotes an exponential variation. If instead the boundary condition is the third kind at $x=0$, we have

$$-k\frac{\partial T'}{\partial x}(0,t)=h_1\left(T_\infty\mathrm{e}^{\left(\frac{\eta_n}{W}\right)^2\alpha t}-T'(0,t)\right) \tag{20b}$$

This problem is denoted $X3JB40T0$. Both of these problems, Eqs. (20a) and (20b) have an exponentially-increasing temporal boundary condition at $x=0$. For both cases we can write the formal solution:

$$\begin{aligned}T'_{XIJB40T0}(x,t)&=\frac{\alpha}{k}H_1\int_{\tau=0}^{t}\mathrm{e}^{\left(\frac{\eta_n}{W}\right)^2\alpha\tau}G_{XIJ}(x,0,t-\tau)\,\mathrm{d}\tau\\&=\frac{\alpha}{k}H_1\mathrm{e}^{\left(\frac{\eta_n}{W}\right)^2\alpha t}\int_{u=0}^{t}\mathrm{e}^{-\left(\frac{\eta_n}{W}\right)^2\alpha u}G_{XIJ}(x,0,u)\,\mathrm{d}u,\\u&=t-\tau\end{aligned} \tag{21}$$

The solution using the long cotime GF is

$$\begin{aligned}T'_{XIJB40T0}(x,t)=&\frac{1}{k}H_1\mathrm{e}^{\left(\frac{\eta_n}{W}\right)^2\alpha t}\\&\times\sum_{m=0}^{\infty}\frac{X_m(x)X_m(0)}{N_{x,m}\left[\left(\frac{\beta_m}{L}\right)^2+\left(\frac{\eta_n}{W}\right)^2\right]}\left(1-\mathrm{e}^{-\left[\left(\frac{\beta_m}{L}\right)^2+\left(\frac{\eta_n}{W}\right)^2\right]\alpha t}\right)\end{aligned} \tag{22}$$

where $H_1=q_1$ for boundary conditions of the second kind and $H_1=h_1T_\infty$ for boundary conditions of the third kind. The 1D solution given by Eq. (22) has quasi-steady and complementary transient components. Both parts are proportional to $\exp(\eta_n^2\alpha t/W^2)$. The quasi-steady-state part is given by the product of this exponential function of time multiplied by a spatial function in series form. To isolate the spatial function, apply the following transformation:

$$T'(x,t)=\frac{H_1L}{k}\mathrm{e}^{\left(\frac{\eta_n}{W}\right)^2\alpha t}\phi_n(x,t) \tag{23}$$

The 1D transient heat conduction equation is

$$\frac{\partial^2T'}{\partial x^2}=\frac{1}{\alpha}\frac{\partial T'}{\partial t} \tag{24}$$

By using the transformation given by Eq. (23) the heat conduction equation becomes

$$\frac{\partial^2\phi_n}{\partial(x^+)^2}=\frac{1}{\alpha}\frac{\partial\phi_n}{\partial t}+C_n^2\phi_n \tag{25}$$

where $x^+=x/L$ and $C_n=\eta_nL/W$. Eq. (25) describes transient heat conduction in a fin, with $XFIJ$ where the F denotes fin. A fin aligned with the x-axis has primary heat conduction along x with sideways-directed heat loss described by the "fin" term $C_n^2\phi_n$ in Eq. (25). The physical connection to the 2D problem is that the "side" losses are associated with the boundary conditions at $y=0$ and $y=W$ which cause the exact character of the y-direction eigenvalue η_n.

It is now the objective to find the steady-state solution to this fin problem. The steady-state form of Eq. (25) is

$$\frac{\mathrm{d}^2\phi_n}{\mathrm{d}(x^+)^2}=C_n^2\phi_n \tag{26}$$

When the boundary condition is of the second kind, Eq. (20a) is transformed to

$$-\frac{\mathrm{d}\phi_n}{\mathrm{d}x^+}(0,t)=1 \tag{27a}$$

The boundary condition at $x=L$ is homogeneous; whatever kind it is in T, it is the same in ϕ_n. If the boundary

condition given by Eq. (27a) is present and $\phi_n = 0$ at $x = L$, the notation for ϕ_n is $XF21B10$.

If the boundary condition at $x = 0$ is of the third kind, transform Eq. (20b) to obtain

$$-\frac{d\phi_n}{dx^+}(0,t) = 1 - Bi_1\phi_n(0,t), \quad Bi_1 = \frac{h_1 L}{k} \tag{27b}$$

The important point is that ϕ_n satisfies an ordinary differential equation which may be solved by non-series means. Solutions for some steady-state ϕ_n problems are given in Appendix B. For example, for case $XF11B10$, the ϕ_n function is given by

$$\phi_n = \frac{e^{-C_n x^+} - e^{-C_n(2-x^+)}}{1 - e^{-2C_n}} \tag{28a}$$

and $H_1 L/k$ in Eq. (23) is replaced by the surface temperature at $x = 0$ which can be denoted as T_0. Another case is for a constant heat flux at $x = 0$ and a zero temperature at $x = L$, denoted $XF21B10$, which has the ϕ_n function

$$\phi_n = \frac{1}{C_n}\frac{e^{-C_n x^+} - e^{-C_n(2-x^+)}}{1 + e^{-2C_n}} \tag{28b}$$

Suppose an algebraic expression for ϕ_n has been obtained. Then the quasi-steady-state part of Eq. (22) equated to Eq. (23) yields

$$\frac{1}{L}e^{(\frac{\eta_n}{W})^2\alpha t}\sum_{m=0}^{\infty}\frac{X_m(x)X_m(0)}{N_{x,m}\left[\left(\frac{\beta_m}{L}\right)^2 + \left(\frac{\eta_n}{W}\right)^2\right]} = e^{(\frac{\eta_n}{W})^2\alpha t}\phi_n(x) \tag{29a}$$

Then the single summation in Eq. (29a) can be given as

$$\frac{1}{L}\sum_{m=0}^{\infty}\frac{X_m(x)X_m(0)}{N_{x,m}\left[\left(\frac{\beta_m}{L}\right)^2 + \left(\frac{\eta_n}{W}\right)^2\right]} = \phi_n(x) \tag{29b}$$

The non-series form on the right of this equation, $\phi_n(x)$, is then used to reduce the 2D GF double-summation to a single-summation. This procedure has the effect of having the eigenvalue problem aligned in the homogeneous direction and also having the hyperbolic functions in the direction of the non-homogeneous boundary condition. It gives the same result as the standard separation of variables approach.

To better compare the final solutions using the two different methods, consider the steady-state of the $X21B10\,Y21B00T0$ example, solved in Section 3. Eq. (14a) can also be written in the form

$$\begin{aligned} T(x,y) &= \sum_{n=1}^{\infty}\left\{\frac{q_1 L}{k}\frac{1}{L}\sum_{m=1}^{\infty}\frac{X_m(x)X_m(0)}{N_{x,m}\left[\left(\frac{\beta_m}{L}\right)^2 + \left(\frac{\eta_n}{W}\right)^2\right]}\right\}\frac{Y_n(y)IY_n}{N_{y,n}} \\ &= \frac{q_1 L}{k}\sum_{n=1}^{\infty}\phi_n\frac{Y_n(y)IY_n}{N_{y,n}} \end{aligned} \tag{30a}$$

where Eq. (28b) is used. Now for the $Y21$ case, we have [12, p. 99]

$$\begin{aligned} &Y_{Y21}(y) = \cos(\eta_n y^+), \quad \eta_n = (n - 1/2)\pi, \\ &N_{y,n} = W/2, \quad IY_{Y21} = (-1)^{n+1}W/\eta_n \end{aligned} \tag{30b}$$

Using Eq. (30b) in Eq. (30a) and also using Eq. (28b) yields the standard result of

$$\begin{aligned} T(x,y) &= 2\frac{q_1 L}{k}\sum_{n=1}^{\infty}\left\{\frac{1}{\eta_n L/W}\frac{e^{-\eta_n\frac{L}{W}x^+} - e^{-\eta_n\frac{L}{W}(2-x^+)}}{1 + e^{-2\eta_n\frac{L}{W}}}\right\} \\ &\quad\times\frac{\cos(\eta_n y^+)(-1)^{n+1}}{\eta_n} \\ &= 2\frac{q_1 W}{k}\sum_{n=1}^{\infty}\frac{e^{-\eta_n\frac{L}{W}x^+} - e^{-\eta_n\frac{L}{W}(2-x^+)}}{1 + e^{-2\eta_n\frac{L}{W}}}\frac{\cos(\eta_n y^+)(-1)^{n+1}}{\eta_n^2} \end{aligned} \tag{31}$$

Analogous to Eq. (18a), the required number of terms is

$$n_{\max} = \frac{R}{\pi}\frac{W}{L}\frac{1}{x^+} + \frac{1}{2} \tag{32}$$

This equation indicates that the number of terms goes to infinity as x^+ goes to zero; that is not correct because Eq. (31) is also divided by η_n^2.which gives a very slow algebraic convergence as x^+ goes to zero. When the heat flux at x^+ at or near zero is needed, the convergence is extremely poor; to demonstrate this point, using Eq. (31) the heat flux at $x^+ = 0$ is

$$\frac{q_x(0,y^+)}{q_1} = \sum_{n=1}^{\infty}\frac{(-1)^{n+1}\cos(\eta_n y^+)}{\eta_n} \tag{33}$$

Numerical values are discussed below. Since Eq. (33) converges poorly at $x = 0$ which is the heated surface and the most important one, Eq. (31) is inferior to Eq. (17a) in that respect. More details on the convergence are given in the next section.

5. Comparison of numerical values

In this section numerical and graphical results are given to compare the two methods of solution for the $X21B10\,Y21B00$ steady-state example. Table 2 is a tabulation of numerical values for Eqs. (17a) and (31). The first column is the L/W aspect ratio; the next two columns give the location of the point; the fourth column gives the number of terms used in the series; and the last two columns give the dimensionless temperatures based on the W dimension. The non-standard solution, Eq. (17a), is in the fifth column; the standard solution. Eq. (31), is in the sixth column. Inaccurate digits are underlined. Some points are now made.

The first point is that intrinsic verification [11] can be observed. The forms of the two summations are different and yet give the same (to 10 digits) converged numerical values. The location $x^+ = y^+ = 0.5$ for $L/W = 1$ is a good point to consider since it does not favor either equation. Slightly over 10 terms in the summation produce the same numerical value of 0.2039147754 which thus has a high probability of being correct and is an indication of intrinsic verification.

The second point is that the Eq. (17a) values (the non-standard solution) for $x^+ = 0$ converge much more rapidly

Table 2
Numerical values for the temperatures given by Eqs. (17a) and (31), non-standard and standard equations, respectively

$\frac{L}{W}$	$\frac{x}{L}$	$\frac{y}{W}$	No. terms	Nonstandard $\left.\frac{T(x,y)}{q_1 W/k}\right\|_{\text{Eq. (17a)}}$	Standard $\left.\frac{T(x,y)}{q_1 W/k}\right\|_{\text{Eq. (31)}}$
1.00	0.000	0.000	1	0.6769582252	0.7434156818
1.00	0.000	0.000	10	0.6753144833	0.6743087186
1.00	0.000	0.000	1000	0.6753144833	0.6753143820
1.00	0.000	0.500	10	0.5627669828	0.5641698500
1.00	0.000	0.500	100	0.5627669827	0.5627526569
1.00	0.000	0.500	1000	0.5627669827	0.5627668394
1.00	0.000	0.999	100	0.0060075818	0.0040709778
1.00	0.000	0.999	1000	0.0050842784	0.0051293631
1.00	0.000	0.999	10000	0.0050824646	0.0050818234
1.00	0.000	0.999	COND3D	0.005082464593	
1.00	0.500	0.000	10	0.2727364660	0.2727364659
1.00	0.500	0.000	30	0.2727364660	0.2727364660
1.00	0.500	0.500	10	0.2039147753	0.2039147755
1.00	0.500	0.500	30	0.2039147754	0.2039147754
1.00	0.500	1.000	10	−0.0001362128	0.0000000000
1.00	0.500	1.000	1000	0.0000000001	0.0000000000
0.20	0.000	0.000	1	0.1998741338	0.2465883580
0.20	0.000	0.000	1000	0.1998741338	0.1998740324
5.00	0.000	0.000	100	0.7424535011	0.7424433698
7.50	0.000	0.000	100	0.7424537453	0.7424436140
10.00	0.000	0.000	100	0.7424537454	0.7424436141

than for Eq. (31). See rows 1–9. As expected, Eq. (17a) converges more slowly as y^+ goes to the value of one. The difficult case of $y^+ = 0.999$ is displayed in rows 7–9 with a comparison of the results given by COND3D [13]. (COND3D is a 3D code for parallelepipeds that uses time-partitioning.) The Eq. (17a) results indicate accuracy to as many digits as given when successive values are the "same." The time-partitioning method used in COND3D indicates accuracy to as many digits as agree when two different (but acceptable) dimensionless partition times are used. (The two values used are $\alpha t_p / L^2 = 0.02$ and 0.05.) The Eq. (17a) value agrees to as many digits as shown. The use of as many terms as 10,000 to get 10 decimal-place accuracy is acceptable. However, the time-partitioning method has an advantage because it uses the same small number of terms in the long cotime component of the solution regardless of the x^+ and y^+ values. An advantage of the method in the present paper is that the cumbersome short-cotime GFs are not needed.

A third point is that the only case in Table 2 for which Eq. (31) is superior is for $y^+ = 1$; in this case the exact value is known to be zero and need not be calculated. Finally some results are given at the point $x^+ = y^+ = 0$ for aspect ratios other than one. For small values of L/W convergence is obtained very quickly for Eq. (17a) as can be inferred from Eq. (18b); see the $L/W = 0.2$ rows in Table 2. As the aspect ratio becomes greater than about 5, the values approach the constant value of 0.7424537454.

A plot of the absolute value of the errors in the dimensionless temperature at $x^+ = 0$ is given by Fig. 2. The non-standard solution errors, Eq. (17a), are considerably smaller than for standard solution errors, Eq. (31); many

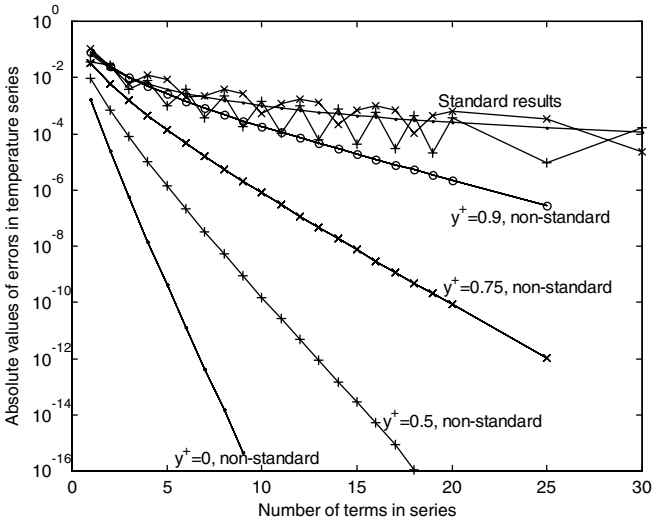

Fig. 2. Absolute values of the errors in the dimensionless temperatures for the $X21B10Y21B00$ steady-state example at $x^+ = 0$ and $L/W = 1$ versus the number of terms in the series. The non-standard results are obtained from Eq. (17a). The standard results are from Eq. (31) and oscillate in sign while the non-standard results do not.

of the errors fluctuate in sign but the non-standard curve for $y^+ = 0$ does not. Fig. 3 displays similar plots for $x^+ = 0.5$. In this plot the curves labeled "Standard results" have errors that are independent of the y/W locations from 0 to 0.9; the non-standard curve for $y^+ = 0.5$ is along the same line. This figure shows that the standard equation, Eq. (31), for $x^+ = 0.5$ and for y^+ greater than 0.5 converges more rapidly than the non-standard equation. However, if only one solution is desired for the steady-state, the

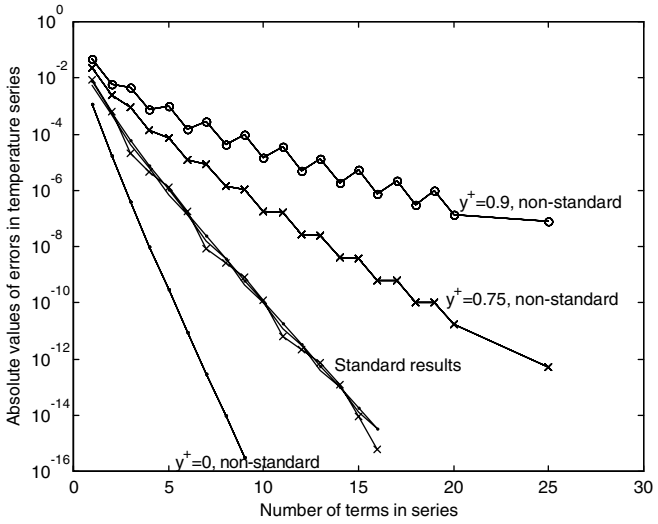

Fig. 3. Absolute values of the errors in the dimensionless temperatures for the *X21B10Y21B00* steady-state example at $x^+ = 0.5$ and $L/W = 1$ versus the number of terms in the series. The non-standard results are obtained from Eq. (17a). The standard results are from Eq. (31).

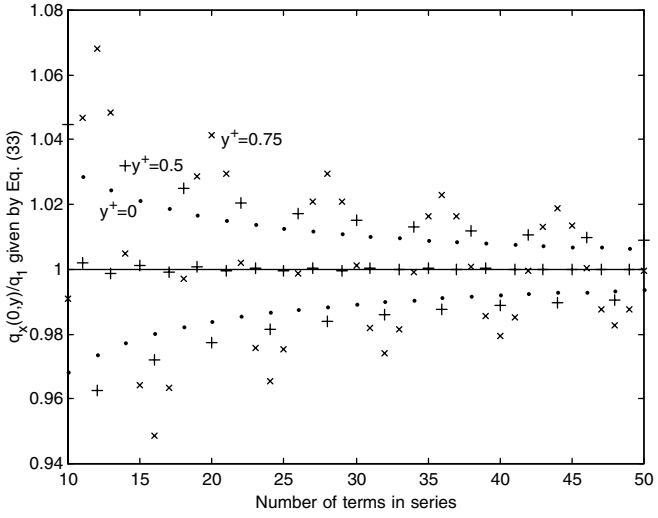

Fig. 4. Heat flux components for the standard equation, Eq. (33), for $x^+ = 0$ as a function in the number of terms. The dots are for $y^+ = 0$; (+) symbols are for $y^+ = 0.5$; and (×) symbols are for $y^+ = 0.75$.

non-standard equation is clearly the better to use. This point is re-enforced by Fig. 4 which shows results for the heat flux at $x^+ = 0$ for the standard solution given by Eq. (33). These values oscillate with the number of terms and very gradually decrease. This is in contrast with the exact heat flux obtained from Eq. (17a) for which the summation is zero at $x^+ = 0$.

6. Equivalent approach: steady 1D GF

In this section an approach is given that is based on steady-state one-dimensional GFs. This approach provides an additional perspective for further insight into the problem. The final results are identical to those already discussed.

Consider the steady-state portion of the original two-dimensional problem, case *XIJB(y-)0YKLB00T0*, for $I = 2$ or 3. The steady-state portion of the solution is given by

$$T(x,y) = \sum_m \sum_n \frac{X_m(x)X_m(0)}{N_{x,m}} W\left[\frac{H_1}{Wk}\frac{Y_n(y)IY_n}{N_{y,n}\left[\frac{\beta_m^2}{L^2}+\frac{\eta_n^2}{W^2}\right]}\right] \tag{34}$$

The elements of the double sum have been arranged to isolate terms that are associated with the x- and y-directions.

6.1. Steady GF solution along y (non-standard solution)

Consider the summation over n, shown in brackets in the above equation, to be the solution of a one-dimensional steady problem along the y-direction. This 1D steady problem may be formally stated with a GF solution [12, p. 66]

$$T(y) = \frac{H_0}{k}\int_{y'=0}^{W}\frac{f(y')}{W}G(y,y')\,dy' \tag{35}$$

This is the steady one-dimensional temperature caused by internal heating of the form $g = H_0 f(y)/W$. By comparing this 1D GF solution with the term in brackets in Eq. (34), the associated one-dimensional steady GF must have the following form:

$$G(y,y') = \sum_n \frac{Y_n(y)Y_n(y')}{N_{y,n}\left[\frac{\beta_m^2}{L^2}+\frac{\eta_n^2}{W^2}\right]} \tag{36}$$

where $Y_n(y)$ is an eigenfunction that satisfies $Y_n''+(\eta_n/W)^2 Y_n = 0$ and appropriate homogeneous boundary conditions at $y = 0$ and $y = W$ (of the same kind as the original 2D problem).

The above GF satisfies the heat conduction equation for a steady fin:

$$\frac{d^2G}{dy^2} - \left(\frac{\beta_m}{L}\right)^2 G + \delta(y-y') = 0 \tag{37}$$

To show that the GF given in Eq. (36) satisfies the above fin equation, differentiate the GF and substitute it into the fin equation, along with the following series form for the Dirac delta function

$$\delta(y-y') = \sum_n \frac{Y_n(y)Y_n(y')}{N_{y,n}} \tag{38}$$

Then the fin equation, Eq. (37), becomes

$$\sum_n \frac{Y_n(y)Y_n(y')}{N_{y,n}}\left\{-\frac{(\eta_n/W)^2}{\left[\frac{\beta_m^2}{L^2}+\frac{\eta_n^2}{W^2}\right]} - \frac{(\beta_m/L)^2}{\left[\frac{\beta_m^2}{L^2}+\frac{\eta_n^2}{W^2}\right]} + 1\right\} = 0 \tag{39}$$

This equation is satisfied for all n, demonstrating that the GF in Eq. (36) satisfies the fin equation.

The next step is to solve the 1D steady heat conduction problem by non-series means. The steady GF method can

be used for this, because the GF is available in an alternate, non-series form.

The GF for the steady-fin cases along the y-direction are designated $YFKL$ where K, $L, = 1,2,3$. The GF for these geometries may be stated in the form of hyperbolic sines and cosines [12, p. 479] or equivalently as exponentials, given by [23]

$$G(y,y') = W\frac{S_2^-(S_1^-\mathrm{e}^{-C_m(2-|y-y'|)/W} + S_1^+\mathrm{e}^{-C_m(2-(y+y')/W)})}{2C_m(S_1^+S_2^+ - S_1^-S_2^-\mathrm{e}^{-2C_m})} + W\frac{S_2^+(S_1^+\mathrm{e}^{-C_m|y-y'|/W} + S_1^-\mathrm{e}^{-C_m(y+y')/W})}{2C_m(S_1^+S_2^+ - S_1^-S_2^-\mathrm{e}^{-2C_m})} \tag{40}$$

Recall that $C_m = \beta_m W/L$. The coefficients depend on the type of boundary conditions at boundaries $j = 1,2$ and are given by

$$S_j^+ = \begin{cases} 1 & \text{side } j \text{ is kind 1 or 2} \\ C_m + Bi_j & \text{side } j \text{ is kind 3} \end{cases}$$
$$S_j^- = \begin{cases} -1 & \text{side } j \text{ is kind 1} \\ 1 & \text{side } j \text{ is kind 2} \\ C_m - Bi_j & \text{side } j \text{ is kind 3} \end{cases} \tag{41}$$

Here $Bi_j = h_j W/k$ is the Biot number at boundary j.

These steady one-dimensional GF may be applied to find the steady temperature. Consider a specific example. For steady case $YF11B00G1$ the GF is given by (use $S_j^+ = 1$ and $S_j^- = -1$)

$$G_{YF11} = W\frac{\mathrm{e}^{-C_m(2-|y-y'|/W)} - \mathrm{e}^{-C_m(2-(y+y')/W)} + \mathrm{e}^{-C_m|y-y'|/W} - \mathrm{e}^{-C_m(y+y')/W}}{2C_m(1-\mathrm{e}^{-2C_m})} \tag{42}$$

and the one-dimensional temperature for $f(y) = 1$ is given by

$$T(y) = \frac{H_1}{k}\int_{y'=0}^{W}\frac{f(y')}{W}G_{YF11}(y,y')\,\mathrm{d}y' = \frac{H_1 W}{k}\frac{1}{C_m^2}\left[1 - \frac{\mathrm{e}^{-C_m y^+} + \mathrm{e}^{-C_m(1-y^+)}}{1+\mathrm{e}^{-C_m}}\right] \tag{43}$$

The final step is to substitute the steady 1D temperature, found by non-series means, into the steady 2D solution to replace one of the summations. The results from the 1D GF approach described here are identical to those from the θ_m procedure described earlier. The relationship between the 1D GF method and the earlier development is a simple proportionality, $T_{\mathrm{FIN}} = \theta_m H_1 W/k$. Thus, the use of steady 1D GF provides another way to find quantity θ_m, some of which are listed in Appendix A.

6.2. Steady GF solution along x (standard solution)

A similar development can be carried out along the x-direction to obtain an alternate single-sum form of the steady 2D solution. Returning to the double-sum steady solution, slightly rearranged

$$T(x,y) = \sum_{m=0}^{\infty}\sum_{n=0}^{\infty}\left[\frac{H_1}{k}\frac{X_m(x)X_m(0)}{N_{x,m}\left[\frac{\beta_m^2}{L^2}+\frac{\eta_n^2}{W^2}\right]}\right]\frac{Y_n(y)IY_n}{N_{y,n}} \tag{44}$$

Consider the sum over m and the term in braces as though it were associated with a one-dimensional solution along x. This one-dimensional steady problem along the x-direction, with a non-homogeneous boundary condition at $x = 0$ of type 2 or 3, may be formally stated with the GF solution:

$$T(x) = \frac{H_1}{k}G(x,x'=0) \tag{45}$$

By comparison with the sum over n in the 2D solution, the steady GF must have the form:

$$G(x,x') = \sum_m \frac{X_m(x)X_m(x')}{N_{x,m}\left[\frac{\beta_m^2}{L^2}+\frac{\eta_n^2}{W^2}\right]} \tag{46}$$

This is a fin-type steady GF along the x-axis which satisfies

$$\frac{\mathrm{d}^2G}{\mathrm{d}x^2} - \left(\frac{\eta_n}{W}\right)^2 G + \delta(x-x') = 0 \tag{47}$$

These steady-fin GF have a non-series form, completely analogous to the y-direction form given earlier; simply replace C_m by C_n, replace y by x, and replace W by L in Eq. (40). Then, the 1D steady, non-series temperature solution in the x-direction may be sought using the steady-fin GF in a manner completely analogous to the y-direction steady-fin GF discussion given above. The only difference is that the appropriate non-homogeneous boundary condition at $x = 0$ must be used.

Finally, the steady-fin temperature solution may be substituted into the 2D steady solution to replace one of the summations. The results are identical to the ϕ_n development given earlier. Thus, the steady GF method provides an alternate method to find functions ϕ_n listed in Appendix B.

6.3. Green's function library and software TFIN

The one-dimensional steady-fin GF given in Eq. (37) are also available at the internet site called the Green's Function Library [24,25]. Individual expressions are given for the nine GF denoted $XFIJ$ for $I = 1,2,3$ and $J = 1,2,3$. In addition, analytical expressions for the fin temperature using the steady-fin GF may be viewed on-line with interactive software TFIN [23]. Software TFIN displays temperature expressions, computed interactively based on user-supplied input values, in the form of MathML expressions (if the web browser is configured appropriately). The displayed MathML expressions may be copied and pasted into commercial mathematics software for evaluation, plotting, etc.

7. Conclusions

Standard separation of variable (SOV) solutions for rectangles heated at a boundary (and in 3D, for parallelepipeds) have poor numerical behavior near the heated boundary, which is often the location of greatest interest. This convergence problem associated with standard SOV solutions has not been directly addressed in any of the advanced heat conduction books (of which we aware, including ours) published over the last five decades. This paper describes a new procedure for developing alternate temperature expressions that have better convergence behavior near the heated boundary.

One new procedure involves only the long-cotime Green's function (GF), making this approach analytically easier than the time-partitioning method for improving convergence, which involves both long-cotime and short-cotime GF. This procedure also provides a way to construct fully-summed forms of certain series expressions, and several examples are given. Another and equivalent procedure is based on steady-state GFs. The solutions developed in this paper can be used along with the standard SOV solutions for checking of numerical values, which we call intrinsic verification, in regions where both solutions are convergent.

Tabulations of algebraic forms for single-summations are given for both the non-standard and standard formulations of the exact solution of the steady-state heat conduction in a rectangle. Appendix A gives the identities for the non-standard formulation and Appendix B for the standard formulation; in both cases the boundary condition is considered to be uniform over the non-homogeneous surface. Although this paper gives methods for deriving these identities, derivations of these known identities need not be repeated. Consequently, the analytical solution of many related problems is considerably simplified. Although the analysis is for the rectangle with non-homogeneous boundary conditions, the method can be extended to other geometries such parallelepipeds and cylinders and to also include volumetric energy generation.

Acknowledgement

The authors appreciate the comments and insights provided by Professors Filippo de Monte and A. Haji-Sheikh, and Dr. Ned Keltner.

Appendix A

Solutions used in the non-standard solution. There are nine cases for a fin-type steady-state equation, *XFIJB*00*G*1, with a constant volumetric energy source. The describing ode is Eq. (12) with $f(y)=1$ and homogeneous boundary conditions. The series is given by Eq. (13). $C_m = \beta_m W/L$

*YF*11*B*00*G*1

$$\theta_m(y) = 2\sum_{n=1}^{\infty} \frac{[\sin(\eta_n y^+)][1/\eta_n]}{\{\frac{1}{2}\}(C_m^2+\eta_n^2)} = \frac{1}{C_m^2}\left[1 - \frac{e^{-C_m y^+} + e^{-C_m(1-y^+)}}{1+e^{-C_m}}\right],$$
$$\eta_n = (2n-1)\pi \tag{A.1}$$

*YF*12*B*00*G*1. For *YF*21*B*00*G*1, replace y^+ by $(1-y^+)$, $\eta_n = \left(n-\frac{1}{2}\right)\pi$.

$$\theta_m(y) = \sum_{n=1}^{\infty} \frac{[\sin(\eta_n y^+)][(1-\cos(\eta_n))/\eta_n]}{\{\frac{1}{2}\}(C_m^2+\eta_n^2)} = \frac{1}{C_m^2}\left[1 - \frac{e^{-C_m y^+} + e^{-C_m(2-y^+)}}{1+e^{-2C_m}}\right] \tag{A.2}$$

*YF*33*B*00*G*1

$$\theta_m(y) = \sum_{n=1}^{\infty} \frac{[\eta_n \cos\left(\eta_n \frac{y}{W}\right) + Bi_1 \sin\left(\eta_n \frac{y}{W}\right)][\sin(\eta_n) + \frac{Bi_1}{\eta_n}(1-\cos(\eta_n))]}{\left\{\frac{1}{2}\left((\eta_n^2+Bi_1^2)\left[1+\frac{Bi_2}{\eta_n^2+Bi_2^2}\right]+Bi_1\right)\right\}(\eta_n^2+C_m^2)}$$
$$\tan(\eta_n) = \frac{\eta_n(Bi_1+Bi_2)}{\eta_n^2 - Bi_1 Bi_2}, \quad Bi_1 = \frac{h_1 W}{k}, \quad Bi_2 = \frac{h_2 W}{k} \tag{A.3}$$

$$\theta_m(y) = \frac{1}{C_m^2}\left[1 - \frac{D_{B1}(e^{-C_m y^+} + D_2 e^{-C_m(2-y^+)}) + D_{B2}(e^{-C_m(1-y^+)} + D_1 e^{-C_m(1+y^+)})}{1 - D_1 D_2 e^{-2C_m}}\right]$$
$$D_j = (C_m - Bi_j)/(C_m + Bi_j), \quad D_{Bj} = Bi_j/(C_m+Bi_j), \quad j = 1,2 \tag{A.4}$$

Appendix B

Solutions for a standard solution. They are for a fin-type steady-state equation, *XFIJB*10, which has 18 possible cases, 9 combinations of boundary conditions for 2 surfaces. The describing differential equation is

$$\frac{d^2\phi_n}{d(x^+)^2} = C_n^2 \phi_n, \quad x^+ = \frac{x}{L}, \quad C_n = \eta_n \frac{L}{W}$$

Various boundary conditions are considered:

$$XF11B10\text{: } \phi_n = \frac{e^{-C_n x^+} - e^{-C_n(2-x^+)}}{1-e^{-2C_n}},$$
$$XF11B01\text{: } \phi_n = \frac{e^{-C_n(1-x^+)} - e^{-C_n(1+x^+)}}{1-e^{-2C_n}},$$
$$XF12B10\text{: } \phi_n = \frac{e^{-C_n x^+} + e^{-C_n(2-x^+)}}{1+e^{-2C_n}},$$
$$XF12B01\text{: } \phi_n = \frac{1}{C_n}\frac{e^{-C_n(1-x^+)} - e^{-C_n(1+x^+)}}{1+e^{-2C_n}},$$
$$XF13B10\text{: } \phi_n = \frac{e^{-C_n x^+} + D_2 e^{-C_n(2-x^+)}}{1+D_2 e^{-2C_n}},$$
$$XF13B01\text{: } \phi_n = D_{R2}\frac{e^{-C_n(1-x^+)} - e^{-C_n(1+x^+)}}{1+D_2 e^{-2C_n}},$$
$$D_2 = (C_n - Bi_2)/(C_n + Bi_2), \quad D_{R2} = 1/(C_n + Bi_2),$$

$$XF21B10:\ \phi_n = \frac{1}{C_n}\frac{e^{-C_n x^+} - e^{-C_n(2-x^+)}}{1+e^{-2C_n}},$$

$$XF21B01:\ \phi_n = \frac{e^{-C_n(1-x^+)} + e^{-C_n(1+x^+)}}{1+e^{-2C_n}},$$

$$XF22B10:\ \phi_n = \frac{1}{C_n}\frac{e^{-C_n x^+} + e^{-C_n(2-x^+)}}{1-e^{-2C_n}},$$

$$XF22B01:\ \phi_n = \frac{1}{C_n}\frac{e^{-C_n(1-x^+)} + e^{-C_n(1+x^+)}}{1-e^{-2C_n}},$$

$$XF23B10:\ \phi_n = \frac{1}{C_n}\frac{e^{-C_n x^+} + D_2 e^{-C_n(2-x^+)}}{1-D_2 e^{-2C_n}},$$

$$XF23B01:\ \phi_n = D_{R2}\frac{e^{-C_n(1-x^+)} + e^{-C_n(1+x^+)}}{1-D_2 e^{-2C_n}},$$

$$XF31B10:\ \phi_n = D_{R1}\frac{e^{-C_n x^+} - e^{-C_n(2-x^+)}}{1+D_1 e^{-2C_n}},$$

$$XF31B01:\ \phi_n = \frac{e^{-C_n(1-x^+)} + D_1 e^{-C_n(1+x^+)}}{1+D_1 e^{-2C_n}},$$

$$D_1 = (C_n - Bi_1)/(C_n + Bi_1), \quad D_{R1} = 1/(C_n + Bi_1),$$

$$XF32B10:\ \phi_n = D_{R1}\frac{e^{-C_n x^+} + e^{-C_n(2-x^+)}}{1-D_1 e^{-2C_n}},$$

$$XF32B01:\ \phi_n = \frac{e^{-C_n(1-x^+)} + D_1 e^{-C_n(1+x^+)}}{C_n(1-D_1 e^{-2C_n})},$$

$$XF33B10:\ \phi_n = D_{R1}\frac{e^{-C_n x^+} + D_2 e^{-C_n(2-x^+)}}{1-D_1 D_2 e^{-2C_n}},$$

$$XF33B01:\ \phi_n = D_{R2}\frac{e^{-C_n(1-x^+)} + D_1 e^{-C_n(1+x^+)}}{(1-D_1 D_2 e^{-2C_n})}.$$

References

[1] J.V. Beck, A. Haji-Sheikh, D.E. Amos, D.H.Y. Yen, Verification solution for partial heating of rectangular solid, Int. J. Heat Mass Transfer 47 (2004) 4243–4255.

[2] V.S. Arpaci, Conduction Heat Transfer, Addison-Wesley, Reading, MA, 1966, p. 194.

[3] M.N. Ozisik, Heat Conduction, second ed., John Wiley, 1993, p. 77.

[4] S. Kakac, Y. Yener, Heat Conduction, third ed., Taylor and Francis, 1993, p. 145.

[5] B. Gebhart, Heat Conduction and Mass Diffusion, McGraw-Hill, New York, 1993, p. 101.

[6] F.P. Incropera, D.P. DeWitt, Introduction to Heat Transfer, third ed., John Wiley, 1996, p. 164.

[7] H.S. Carslaw, Fourier's Series and Integrals, Macmillan, 1930.

[8] G.E. Myers, Analytical Methods in Heat Conduction, Genium Publishing, 1987, Section 3.2.

[9] K.D. Cole, D.H.Y. Yen, Green's functions, temperature, and heat flux in the rectangle, Int. J. Heat Mass Transfer 44 (20) (2001) 3883–3894.

[10] P.E. Crittenden, K.D. Cole, Fast-converging steady-state heat conduction in the rectangular parallelepiped, Int. J. Heat Mass Transfer 45 (2002) 3585–3596.

[11] J.V. Beck, R. McMasters, K.J. Dowding, D.E. Amos, Intrinsic verification methods in linear heat conduction, Int. J. Heat Mass Transfer 49 (2006) 2984–2994.

[12] J.V. Beck, K.D. Cole, A. Haji-Sheikh, B. Litkouhi, Heat Conduction Using Green's Functions, Hemisphere Publishing Corp., New York, 1992.

[13] R. McMasters, K. Dowding, J. Beck, D. Yen, Methodology to generate accurate solutions for verification in transient three-dimensional heat conduction, Numer. Heat Transfer, Part B: Fundamentals 41 (6) (2002) 521–541.

[14] J.V. Beck, R.L. McMasters, Solutions for multi-dimensional transient heat conduction with solid body motion, Int. J. Heat Mass Transfer 47 (17–18) (2004) 3757–3768.

[15] D.H.Y. Yen, J. Beck, R. McMasters, D.E. Amos, Solution of an initial-boundary value problem for heat conduction in a parallelepiped by time partitioning, Int. J. Heat Mass Transfer 45 (2002) 4267–4279.

[16] F. de Monte, Transient heat conduction in a one-dimensional composite slab. A 'natural' analytic approach, Int. J. Heat Mass Transfer 43 (19) (2000) 3607–3619.

[17] F. de Monte, Unsteady heat conduction in two-dimensional two slab-shaped regions. Exact closed-form solution and results, Int. J. Heat Mass Transfer 46 (8) (2003) 1455–1469.

[18] X. Lu, P. Tervola, M. Viljanen, Transient analytical solution to heat conduction in composite cylinder, Int. J. Heat Mass Transfer 49 (1–2) (2006) 341–348.

[19] X. Lu, P. Tervola, M. Viljanen, Transient analytical solution to heat conduction in multi-dimensional composite cylinder slab, Int. J. Heat Mass Transfer 49 (5–6) (2006) 1107–1114.

[20] R.C. Xin, W.O. Tao, Analytical solution for transient heat conduction in two semi-infinite bodies in contact, J. Heat Transfer 116 (1994) 224–228.

[21] A. Azimi, S. Kazemzadeh Hannani, B. Farhanieh, Structured multiblock grid solution of two-dimensional transient inverse heat conduction problems in cartesian coordinate system, Numer. Heat Transfer, Part B: Fundamentals 48 (6) (2006) 571–590.

[22] T. Luttich, A. Mhamdi, W. Marquardt, Design, formulation, and solution of multidimensional inverse heat conduction problems, Numer. Heat Transfer, Part B: Fundamentals 47 (2) (2005) 111–133.

[23] K.D. Cole, Computer software for fins and slab bodies with Green's functions, Comput. Appl. Eng. Educ. 12 (3) (2004) 189–197.

[24] K.D. Cole, P.E. Crittenden, Heat conduction in cartesian coordinates and a library of Green's functions, in: Proceedings of the 35th National Heat Transfer Conference, Anaheim, CA, June 10–12, 2001.

[25] K.D. Cole, Green's Function Library. Available from: <http://www.greensfunction.unl.edu>.